

Original Research

Contrasting Spectroscopic Characterization and Environmental Behavior of Dissolved Organic Matter in Shallow and Deep Mine Water of Shendong Mining Area, China

Chunming Hao^{1,2,3}, Kaikai He², Chao Liu⁴, Yantang Wang², Herong Gui^{3*}

¹State Key Laboratory of Coal Resources and Safe Mining, Beijing, 100081, P.R. China

²North China Institute of Science and Technology, Hebei, 065201, P.R. China

³Key Laboratory of Mine Water Resource Utilization of Anhui Higher Education Institutes, Suzhou University, Anhui, 234000, P.R. China

⁴Liaoning Metallurgical Geological Exploration Research Institute Co., LTD, Anshan, 114038, P.R. China

Received: 24 March 2023

Accepted: 4 May 2023

Abstract

Underground reservoirs have been widely used to facilitate mine water storage in the Shendong mining area. Unfortunately, problems with suspended matter and soluble pollutants in underground reservoir water have occurred. However, as indicators of the mine water environment, the spectroscopic characteristics, geochemical sources of dissolved organic matter (DOM), and influence on the hydrochemistry of mine water remain unclear. In this study, DOM concentration was revealed in the mine water of Shendong mining area, ranging from 0.12 mg/L to 4.90 mg/L, with a mean value of 0.93 mg/L. EEM-PARAFAC models and spectral parameter analysis identified autochthonous components and terrestrial substances that dominated shallow and deep mine water DOM, respectively. Compared with shallow mine water, DOM had lower degrees of humification and more freshly terrestrial substances with higher biological index (BIX), and humification index (HIX), lower E2/E3 ratio, and a254 values in deep mine water owing to emulsion oil leakage. The DOM spectral parameters were helpful in conveniently monitoring the change in mine water quality (total dissolved solids (TDS) and total nitrogen (TN)) by significant correlation.

Keywords: dissolved organic matter, fluorescence, terrestrial substances, hydrochemistry, mine water

Introduction

Dissolved organic matter (DOM) is a heterogeneous mixture of aromatic and aliphatic organic compounds, mainly consisting of humic compounds, proteins, carbohydrates, and aromatic compounds [1-4]. Generally, DOM originates from natural sources, including soil organic matter, sediment, microorganisms, algae, and plant degradation [5, 6]. Anthropogenic activities such as the use of fluorescent detergent components and pollutant discharge from industries, agriculture, and households also contribute a significant amount of DOM to aquatic environments [6, 7]. In natural oxic water, DOM is important for the geochemical and photochemical cycles of nutrient elements such as C, N, P, and S [1, 5, 8]. DOM also plays a key role in the transport and transformation of organic pollutants and trace metals in aquatic systems [2, 4, 9, 10].

Excitation-emission matrices (EEM) are sensitive and powerful techniques for characterising DOM in natural water, providing a three-dimensional fluorescence landscape [11, 12]. Parallel factor analysis (PARAFAC) is extensively used to identify individual fluorescent components of DOM by combining EEM spectroscopy to probe clear and complete information about organic substances in complex materials [11, 12]. Recently, EEM spectroscopy using PARAFAC analysis has been successfully applied for the identification of components, sources, and pollutant binding properties of DOM owing to its high sensitivity and efficiency [4, 11, 13]. Fluorescent indices, such as the spectral slope ratio (S_R), fluorescence index (FI), biological index (BIX), and humification index (HIX), have been widely used to trace the origin and transformation of DOM from various sources [14-17].

As one of the eight largest coalfields in the world, Shendong mining area has reserves amounting to 223.6 billion tons [18, 19]. Under the exploitation of high-intensity coal resources, approximately 31 million tons of mine water are produced annually in the Shendong mining area, of which only about 25% is utilized [20, 21]. Generally, unexploited mine water is discharged into rivers or directly on the land surface, polluting local aquatic ecosystems and threatening local human health [20, 22, 23]. To solve this problem, underground reservoirs have been widely applied in the Shendong mining area, facilitating the storage of mine water in the open voids between the broken rock masses [24, 25]. Meanwhile, the mine water stored in underground reservoirs can supply water for industry and domestic use in the Shendong mining area after purification [19, 20, 26]. Mine water environment protection in underground reservoirs should be considered to maximize the ecological and resident benefits for Shendong mining area. Unfortunately, mine water contains large amounts of suspended matter and soluble pollutants, including heavy metals and other harmful organic substances as a result of dissolution and

leaching effects. Studies have also been conducted on the spatial distributions, polluted source, and formation mechanisms of fluorite [18, 22], DOM [27, 28], salinity [20], and nitrate [23, 29, 30]. As an indicator of the mine water environment, the spectroscopic characteristics and geochemical sources of DOM attract global attention. As the major components of the terrestrial derived DOM, protein-like substances widespread and contributes with 13.75-16.41 mg/L in Shendong mine water [27, 28]. However, the influence of hydrogeochemical factors on the optical properties of DOM in mine water remains unclear.

Therefore, this study mainly aims to: 1) investigate the spectroscopic characteristics and geochemical sources of DOM in mine water by fluorescence PARAFAC; 2) compare the DOM chemical properties and geochemical behaviors between shallow and deep mine water; 3) reveal the relationship between DOM and geochemical elements in shallow and deep mine water. This research will help us to better manage and monitor mine water for protecting ecosystem in the study region.

Methods

Study Area

The Shendong mining area is located in the contiguous area between the Maowusu Sandy Land and the Loess Plateau at the border of Shaanxi, Inner Mongolia, and Shanxi provinces, with an area of 3356.11 km². The mining area is situated in a typical semi-arid and semi-desert plateau continental climate with a mean annual temperature of approximately 11.20°C [18, 25]. The average annual rainfall over many years is approximately 320-440 mm. However, the average annual evaporation reaches 2297.40-2838.70 mm, with a large yearly variation and an erratic seasonal distribution. The area has a loose composition of surface material, sparse vegetation, and flowing and semifixed sand [19, 26]. Moreover, there are two main rivers: the Ulan Mulun River and Grotto River.

The minable coal seams in the J_{1-2y} strata include No.1⁻², 2⁻², 3⁻¹, 4⁻², and 5⁻² coal seams, with burial depths varying from 60 to 400 m and an average thickness of 4-6 m in Shendong mining area. The mine water mainly originates from the J_{1-2y} aquifers, where stored abundant coal resources [18, 22, 26]. Generally, mass groundwater within the J_{1-2y} aquifers exerts degrees of leakage, gathers into the goaf, and becomes mine water during large-scale and high-intensity coal mining. To effectively alleviate water shortages and elevate mine water efficiency, thirty-five underground reservoirs were built in the study area in September 2015 [20, 21]. The total maximum storage capacity of mine water for the underground reservoirs of the Shendong mine reached 31 million m³ [29]. The Shendong mining

area uses recycled water resources accumulated in underground reservoirs to supply adequate water for the surrounding industrial, domestic, and ecological demands. Previous studies have verified that mine water is polluted by coal and coal gangues in some underground reservoirs during its frequent storage and transport [18, 25, 27, 31].

Sample Collection and Analysis

In order to evaluate the DOM levels in mine water, 38 mine water samples were collected from underground reservoirs in underground coal mines in June 2022, following with Technical specifications for environmental monitoring of groundwater (HJ 164-2020) (Fig. 1). Before sample collection, brown high-density polyethylene (HDPE) bottles were flushed with distilled water and sample water two or three times. Each collected mine water sample was filtered using a Jinteng filter with a 0.45 μm glass fibre membrane. The filtered sample was then divided into two 500 ml bottles of water and collected for major ion analysis (F^- and Total nitrogen (TN)) and DOM, respectively.

DOM was measured using a total organic carbon analyser (TOC-5000, Japan) with an analytical precision of $\pm 2\%$. The fluorescence characteristics of the mine water samples were measured by three-dimensional fluorescence spectrophotometry (F7000, Japan) with excitation and emission slit bandwidths of 5 nm, scanning speed of 500 nm/min, and excitation (Ex) was 250-450 nm with an emission scanning range of 220-520 nm [2, 32]. Fluorescence intensities and DOM values were obtained according to the methods described by Malik et al. [2], Kulkarni et al. [33], and Kulkarni and Mladenov et al. [10].

The absorption coefficient at 254 nm (a_{254}) is important for the analysis of the relative content of DOM [8, 34]. The DOM absorption ratio, $E2:E3$, was calculated using the absorbance at 250 nm and 365 nm and was used to monitor the changes in molecular weight [35]. The ratio of spectral slopes in the wavelength regions of 275–295 nm ($S_{275-295}$) and 350–400 nm ($S_{350-400}$), known as S_R , can be found to indicate phytoplankton activity and is negatively correlated with the molecular weight of DOM [34-36]. The a_{254} and S_R details of the calculation process are detailed in Jiang et al. [3] and Ren et al. [34], respectively.

The EEM spectral parameter, FI, was calculated as the ratio of the fluorescence intensities at emission wavelengths of 450 and 500 nm, at an excitation of 370 nm, reflecting the origin of humic substances in DOM [1, 4]. HIX is the ratio of the integrals of fluorescence over the emission wavelengths of 435-480 nm divided by 300-445 nm, at a constant excitation wavelength of 254 nm, indicating the degree of DOM humification [3, 5, 36]. Additionally, as an indicator of the contribution of recently microbially

produced DOM, BIX was computed using an excitation wavelength of 310 nm for the ratio of fluorescence intensity at emission wavelengths of 420-435nm. $\beta:\alpha$ was also calculated from the ratio of fluorescence intensity at emission wavelengths of 380 nm and 420-435 nm with an excitation wavelength of 370 nm [2, 6].

The concentrations of F^- were determined by ion chromatography (Dionex Integrion IC, Thermo Fisher, USA). TN was measured using the potassium persulfate digestion method based on alkaline potassium peroxydisulfate [12, 37]. The pH and total dissolved solids (TDS) were measured during sample collection using a portable pH meter (HANNA H18424) and a portable conductivity meter (HANNA H1833), respectively.

Statistical Analysis

The significant differences between data ($p < 0.05$) were analysed using the t-test and one-way ANOVA. PARAFAC model analysis and spectral indices, including FI, HIX, BIX, a_{254} , S_R , and $\beta:\alpha$ of EEM data were carried out in MATLAB 2012a (Natick, MA, USA) using the DOM Fluor v.1.7 toolbox and EFC v1.2 software, respectively [3, 32]. Descriptive data, such as the mean, range, standard deviation, Spearman correlation analysis, and principal component analysis (PCA), were analysed using Origin 2022 (Northampton, MA, USA).

Results and Discussion

Characteristics of Mine Water Quality Indicators

The geochemical data for the mine water samples from the Shendong mining area are presented in Table 1. The analysed samples had neutral to basic pH ranging from 7.02 to 9.00 with a mean value of 7.54, indicating a weakly alkaline and alkaline environment of the mine water. The TDS concentrations varied from 195 to 5077 mg/L (mean 1100 mg/L), and approximately 39.47% of the samples had TDS values above 1000 mg/L, exceeding China's national drinking water quality guidelines. The range of TN and F^- concentrations was 0.16-10.40 mg/L and 0.04-7.81 mg/L, with mean value of 0.69 mg/L and 3.76 mg/L, respectively. Notably, 63.16% of the mine water samples had elevated F^- concentrations that exceeded China's national standards (1.00 mg/L) for drinking water. These results are similar to those reported by Hao et al. [3, 32] and Zhang et al. [25].

A large variation of DOM concentration was revealed in shallow mine water, ranging from 0.14 mg/L to 4.90 mg/L, with a mean value of 1.08 mg/L; while the DOM concentrations changed from 0.12 mg/L to 3.76 mg/L, with a mean value of

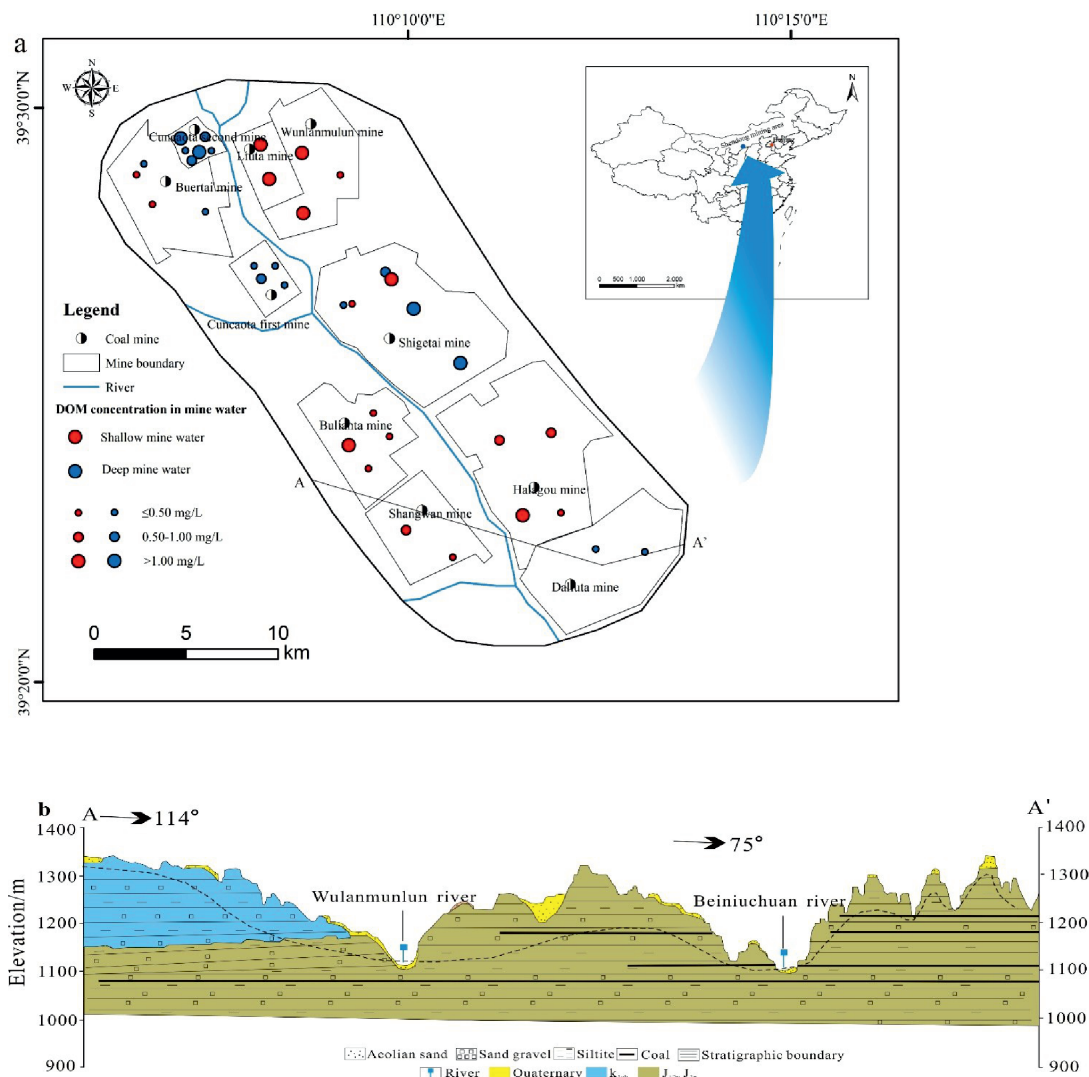


Fig. 1 a) Map of water sampling locations for 19 shallow mine water and 19 deep mine water in the study area; b) Schematic hydrogeological cross-section.

0.79 mg/L in deep mine water (Table 1). The mean DOM concentration of shallow mine water is higher than that of deep mine water, suggesting that shallow mine water may have more DOM sources [28, 29]. Among these mine water samples, waters of coal mines in the east of Ulan Mulun River had higher DOM concentrations than those of coal mines in the west of Ulan Mulun River, where Wulanmulun mine was the highest, with a DOM of 4.90 mg/L (Fig. 1). Based on the depositional environment and facilitate further analysis, the mine water samples were divided into two groups: 1⁻² and 2⁻² coal seams of mine water are referred to shallow mine water and 3⁻¹, 4⁻², and 5⁻² coal seams of mine water are named as deep mine water, respectively.

Fig. 2a) indicates that higher DOM mine water samples is enriched ranging from -50 to -200 m depth. In contrast, the mine water with depth more than 200 m had low DOM. Compared with shallow mine water, the DOM concentration slightly decreased in deep mine water (Fig. 2b); the mean DOM concentration

in shallow mine water was 1.36 times that in deep mine water. These results indicate that the near-surface environment and low burial depth may contribute to increased DOM concentrations [28, 38].

UV-Vis Absorption Spectroscopy Characteristics of DOM in Mine Water

As shown in Fig. 3a), a_{254} values in shallow mine water (mean 6.79 m^{-1}) were significantly greater than those in deep mine water (mean = 4.92 m^{-1} ; $p < 0.05$). In addition, the E2/E3 ratio of shallow mine water showed a higher mean value than that of deep mine water, indicating a decrease in humification and aromatisation in shallow mine water [9, 35]. The E2/E3 ratio values varied more broadly in shallow mine water, which might be explained by a significant contribution from multiple DOM sources owing to the near-surface environment [1, 39]. A similar trend was observed along the gradient for the S_R ratio in shallow and deep mine

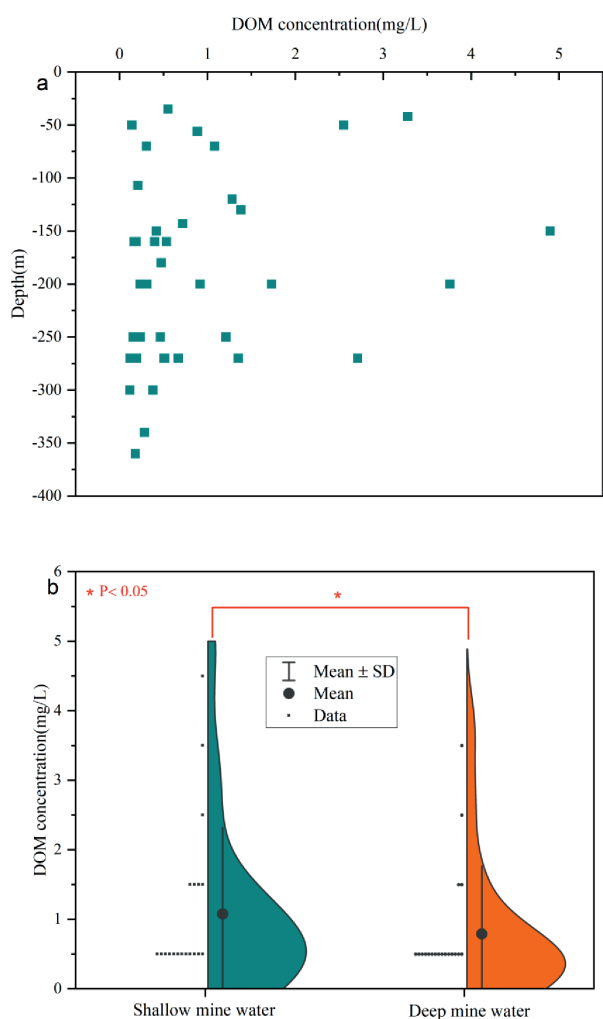


Fig. 2. a) Variation in DOM concentration in mine water with depth; b) Box-whisker diagrams of dissolved organic matter (DOM) in shallow and deep mine water.

water, suggesting no obvious differences in molecular weight compounds were found [11, 35, 40]. This suggests a similar contribution from microbial/algal sources to the DOM signature in shallow and deep mine water. The apparent levels of suspended particles in mine water are caused by turbidity, which may preferentially remove high molecular mass DOM by adsorption onto particles [4]. These UV-Vis absorption spectroscopy parameters showed considerable variability owing to strong individual differences for each sample. Therefore, differences in mining activities and coal resources in the surroundings can lead to a corresponding change in the molecular weight, humification, and aromatisation of DOM [27, 28].

Fluorescence Spectral Characteristic of DOM in Mine Water

The three DOM components were observed using PARAFAC models (Fig. 4 and Table 2). The excitation peak of component 1 (C1) was at 250 nm and its emission peak was at 380 nm, reflecting humic acid-like substances [5, 37]. This component can be identified as a specific humic acid with a low molecular weight that is widely distributed in rivers and agricultural environments [16, 41, 42]. Component 2 (C2) had excitation peaks at 265 nm and an emission peak at 440 nm, representing higher molecular weight humic acid-like structures [11, 16, 36]. Finally, Component 3 (C3) displayed Ex/Em maxima at 280/330 nm, corresponding to protein-like components, which are autochthonous DOM in mine water and are associated with microbial activity [32, 43]. Compared with C1, C2 comprised compounds that were more hydrophobic and larger in molecular size owing to the longer peak of the excitation and emission wavelengths. Thus, C2 is

Table 1. Geochemistry data and spectroscopy parameters of the dissolved organic matter (DOM) in different mine waters in the Shandong mining area.

Types	DOM	F ⁻	TN	TDS	FI	β:α	BIX	HIX	C1	C2	C3	E2/E3	S _r	a254	pH
	mg/L								R.U.					m ⁻¹	
Shallow mine water (n = 19)															
Max	4.90	8.86	0.93	2106	3.74	1.75	1.59	0.89	38.14	24.19	53.36	55.00	7.46	25.79	8.47
Min	0.14	0.16	0.04	207	2.05	0.79	0.01	0.50	2.05	1.93	0.18	0.43	0.02	0.23	7.02
Mean	1.08	2.95	0.26	975	2.60	1.18	1.03	0.68	15.40	9.36	14.92	7.72	1.55	6.80	8.02
SD	1.24	2.99	0.25	630.59	0.41	0.23	0.43	0.11	9.13	5.51	14.38	14.25	2.01	6.75	0.41
Deep mine water (n = 19)															
Max	3.76	10.40	7.81	5077	4.40	1.34	2.26	1.00	32.98	23.27	32.59	12.00	7.69	25.33	9.00
Min	0.12	0.16	0.06	195	2.25	0.01	0.96	0.65	0.00	0.65	0.00	0.09	0.01	0.46	7.20
Mean	0.79	4.57	1.11	1224	3.05	0.85	1.37	0.82	9.75	7.32	7.05	3.46	1.55	4.92	7.92
SD	0.98	3.92	1.79	1147.21	0.71	0.38	0.29	0.10	10.02	6.30	8.68	2.91	1.84	6.29	0.65

Note: Values below the LODs (limits of detection) are set to zero for statistical purposes.

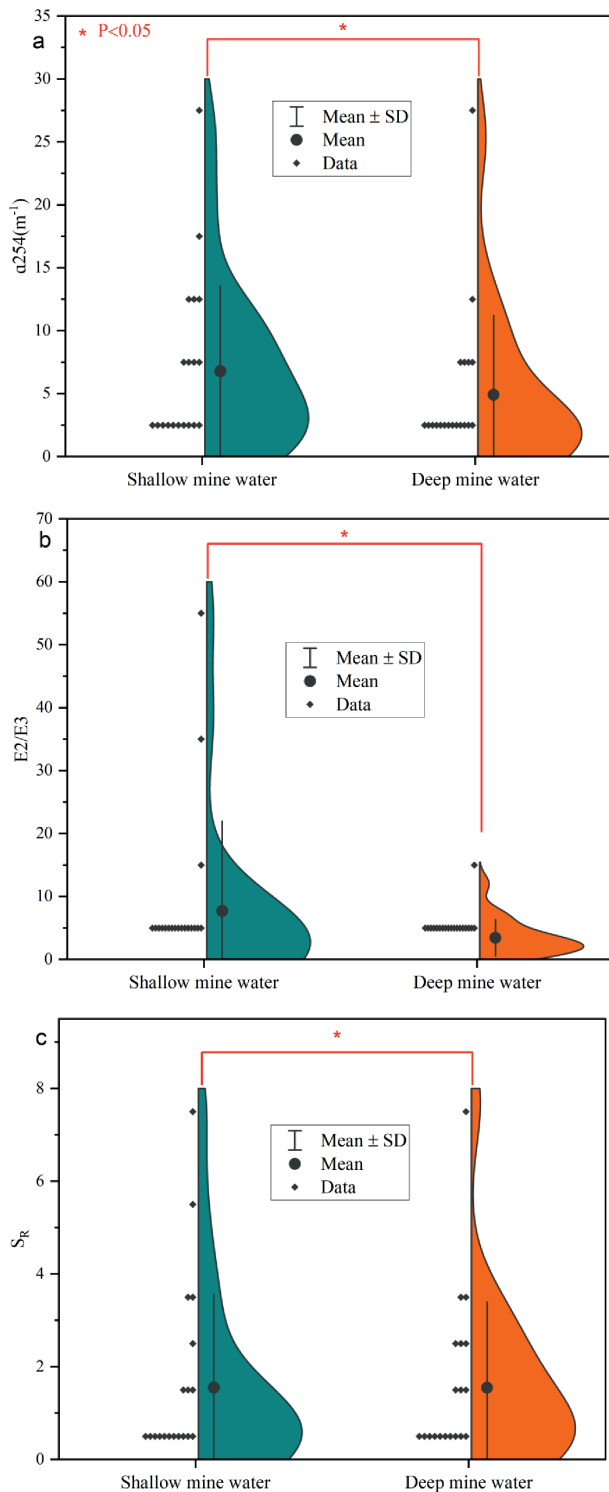


Fig. 3. Box-whisker diagrams of: a) A_{254} ; b) $E2/E3$; c) S_R of DOM in shallow and deep mine water.

usually identified as terrestrial humic acid with a more aromatic structure [44].

The mean component fluorescence intensities (F_{max} (C1), F_{max} (C2), and F_{max} (C3)) were all significantly higher in shallow mine water than in deep mine water, indicating more bioactive DOM in shallow mine water than in deep mine water [43]. In both shallow

and deep mine water, the relative contributions of the sum of humic-like DOM components (C1+C2) were predominant in DOM components (Fig. 5d), indicating that the main components of DOM were humic-like substances. Additionally, C1 was predominant in shallow mine water (mean = 40.79%), followed by C3 (mean = 32.48%) and C2 (mean = 26.73%), whereas C2 was the highest in deep mine water (mean = 40.81%), followed by C1 (mean = 34.52%) and C3 (mean = 24.67%), showing different DOM components [43]. Higher relative contents of C2 and the sum of C1 and C2, and lower relative contents of C1 and C3 were also observed in deep mine water relative to shallow mine water (Fig. 5d), indicating higher molecular weight humic acid-like structures (eg. aromaticity) in deep mine waters.

In this study, all shallow and deep mine water samples showed FI values higher than 1.9, which may be directly attributed to a microbially derived origin [31, 45]. In addition, excess suspended coal in shallow and deep mine waters might have induced higher levels of endogenous protein-like components. The HIX values of the shallow and deep mine water samples were in the range of 0.50-1.00, which was much less than 4, indicating less humification [45]. The reason for the lower humification of DOM in shallow and deep mine water could be explained by two major reasons: (1) terrestrial sources in the Shendong mining area may show an untypically low degree of humification due to the scarce vegetation and vulnerable ecological environment [22]; (2) the coal seam is buried so deep that terrestrial DOM has difficulty infiltrating the mine water through goaf fissures [19, 20]. Additionally, 63.11% of shallow mine water samples and 94.74% of deep mine water samples BIX value has high BIX values (>0.8) for DOM, with an obvious terrestrial component of freshly produced OM of biological or aquatic bacterial origin. Usually, coal mining equipment requires a large amount of emulsion oil to maintain efficient mining in the Shendong Mining Area. These emulsion oils were complex in composition and contained a large amount of autochthonous DOM that could leak into the mine water and elevate the BIX values [27, 28, 46]. Interestingly, slightly higher BIX and HIX values were observed in deep mine water than in shallow mine water (Fig. 6), indicating that DOM had lower degrees of humification and more fresh terrestrial substances in deep mine water, which may be attributed to stronger mining activities and emulsion oil consumed [27]. Deep mine water has lower $\beta:\alpha$ values than shallow mine water, indicating a higher contribution of newly produced microbial DOM components or terrestrial inputs in deep mine water [6, 47]. Usually, $\beta:\alpha$ has the opposite function to microbial degradation [34, 47]. BIX values were in the higher ranges, confirming the production of more microbial-derived terrestrial DOM components in the deep mine water. Meanwhile, more emulsion oil leakage entered the deep mine water and enhanced terrestrial fresh DOM production and microbial activities.

FI had a significant positive correlation with BIX ($R = 0.70$) and $\beta:\alpha$ ($R = 0.73$) in shallow mine water (Fig. 7a), and had a moderate negative correlation with $\beta:\alpha$ ($R = -0.63$) in deep mine water (Fig. 7b), describing the dominance of autochthonous DOM components in shallow mine water and terrestrial substances in deep

mine water, respectively [6]. Meanwhile, HIX had a moderate positive relationship with BIX ($R = 0.58$), the sum of C1 and C2 (0.46) and C2 (0.45) in deep mine water, correspondingly, a weak negative relationship with BIX ($R = -0.03$), the sum of C1 and C2 (-0.26) and C2 (-0.42) in shallow mine water, confirming

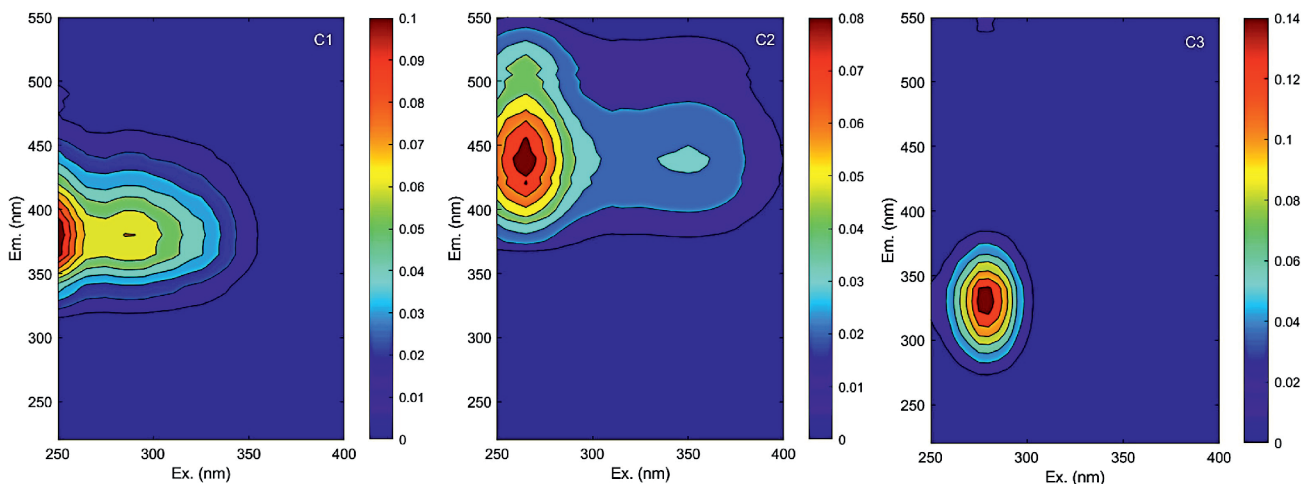


Fig. 4. Spectral characteristics of the three identified DOM components using PARAFAC modeling.

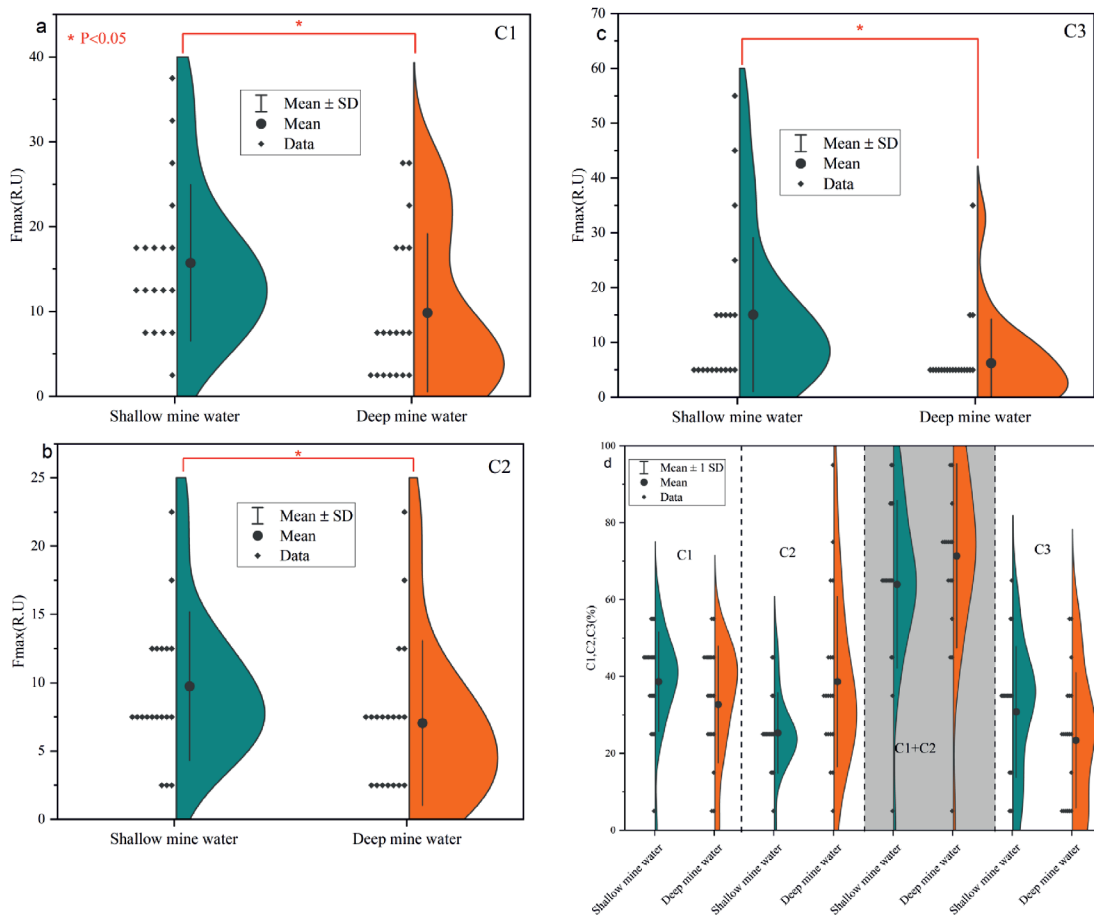


Fig. 5. Box-whisker diagrams of: a) fluorescence intensity of C1; b) fluorescence intensity of C2; c) fluorescence intensity of C3; d) fluorescence intensity of the sum of C1 and C2 of DOM in shallow and deep mine water.

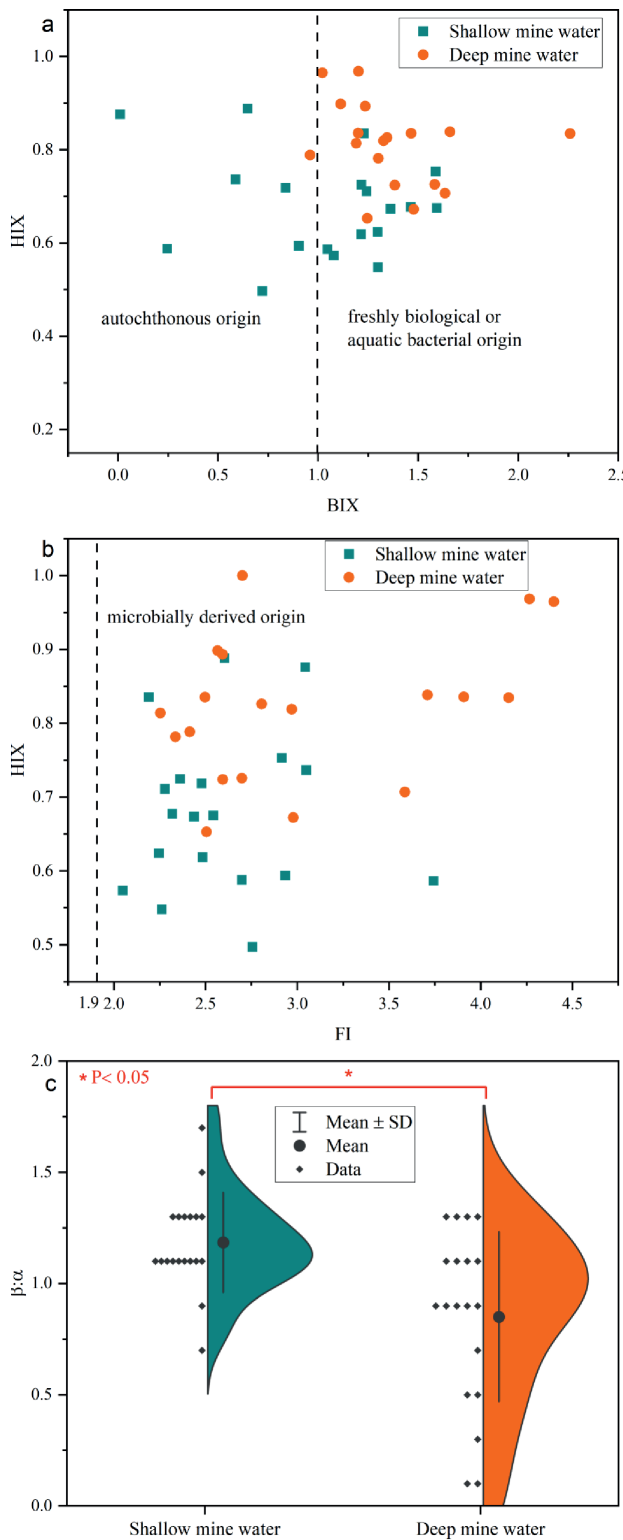


Fig. 6. The plots of the: a) relationship between HIX and BIX; b) relationship between HIX and FI; c) comparison with $\beta:\alpha$ of DOM in shallow and deep mine water.

that higher aromaticity and larger molecular size DOM components facilitated in deep mine water [37]. Moreover, BIX had a strong positive correlation with

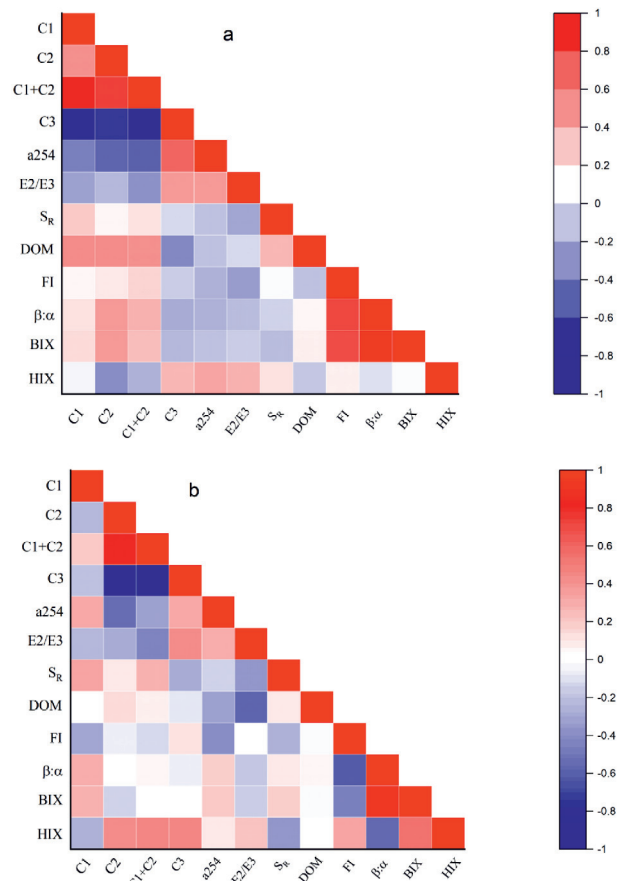


Fig. 7. Correlation between DOM components and spectral parameters: a) in shallow mine water; b) in deep mine water.

$\beta:\alpha$ in shallow ($R = 0.96$) and deep ($R = 0.93$) mine water, indicating low molecular size autochthonous DOM components were ubiquitous in mine water [6].

Relationships between DOM Properties and Hydrochemical Factors in Mine Water

Generally, environmental conditions may be indirectly responsible for the generation of DOM and its corresponding rapid degradation by sunlight-induced and microbial processes [48]. As shown in Fig. 8, environmental factors (F-, TDS, TN, and pH) have a corresponding relationship with UV-Vis absorption spectroscopy and fluorescence spectral parameters of DOM by factors analysis in shallow and deep mine water.

The correlations between F- and C1 and FI were moderately positive and negative in the shallow mine water (Fig. 8a), respectively. Correspondingly, F- was positively correlated with BIX, $\beta:\alpha$, and S_R , and weakly negatively correlated with HIX and DOM in the deep mine water (Fig. 8b). It was observed that concentrations of F- in shallow mine water showed a big variation from 0.16 to 8.86 mg/L (mean 2.95 mg/L), slightly lower than those of deep mine water (from 0.16 to 10.40 mg/L; mean 4.57 mg/L).

Table. 2. Description of the components of the PARAFAC model from water samples.

Component	(Ex/Em)/nm	Description	References
C1	250/380	Humic-like	C2:230(290)/390 (Pi et al. 2015; Li et al. 2019; Sun et al. 2021); 215-280/380-550 (Zhou et al. 2021; Yi et al. 2022)
C2	265/440	Terrestrial fulvic-like	C1:260/400-460 (Singh et al. 2013; Li et al. 2019; Xu et al. 2021)
C3	280/330	Tryptophan-like or protein-like	C4:280,330 (Guo et al. 2019; Hao et al. 2022)

The different relationships proved that DOM properties had minimal impact on the enrichment of F⁻ in shallow and deep mine water, confirming previous studies that DOM can strongly exhibit the environmental behaviours and fates of organic pollutants and trace metals in aquatic systems but has less influence on the toxicity and transport of inorganic halogen elements [6, 14, 49].

TDS had a positive correlation with a 254 and E2/E3, and C1 in the shallow mine water. In contrast, a positive relationship between TDS and E2/E3, HIX, C2, and FI was also found in deep mine water. This phenomenon indicated that the relative content and molecular

weight of DOM were the key factors affecting the salinity of shallow and deep mine water [4]. Previous studies have reported that photodegradation occurs mainly in the high-salinity region, which could induce various DOM biogeochemical removal or production processes. Importantly, DOM content is related to salinity, reflecting water residence times and dissolved matter accumulation within semi-humid and semi-arid regions [36]. The observed trends were the decrease and increase in FI with salinity in shallow and deep mine water, which were probably caused by different microbial activities [48]. Generally, DOM is more sensitive to photochemical and microbial degradation with different sources (terrestrial or autochthonous) and molecular weights, resulting in different relationships between DOM and salinity in shallow and deep mine water. A significant positive correlation with TN, HIX, and C2 was observed in deep mine water, showing that large molecular weight humic acid-like substances (i.e. emulsion oil) were helpful for elevated TN concentrations. To the best of our knowledge, TN, including NH₄⁺-N, NO₃⁻-N, and other forms of nitrogen, generally form complexes with DOM through various complexes [1, 34, 48]. Therefore, an increase in emulsion oil leakage can provide a useful biogeochemical understanding of TN concentrations in deep mine water. Simultaneously, the continuous increase in nutrient content caused by human activities contributed to the increase in DOM quantity and drove the DOM composition to be more protein-like [50, 51]. An inverse correlation between TN and BIX, β:α, can also be a good indicator of the TN favoured in fresh and flowing mine water environments. In contrast, a254 and C3 had strong positive corrections, and FI and C2 had negative corrections with TN in shallow mine water. As mentioned above, C3 is mainly affected by the activity of microorganisms, such as algae. Hence, the effect of biological activities on the water body is either absent or limited, while the input of TN controls the production of C3 and the activity of microorganisms in shallow mine water [50].

Furthermore, pH had no obvious correlations with these indicators in Fig. 8(a,b), and only a254 and FI were correlated with the organic indicators in shallow mine water, indicating that the DOM components were a minor contributor to the pH of shallow and deep mine water.

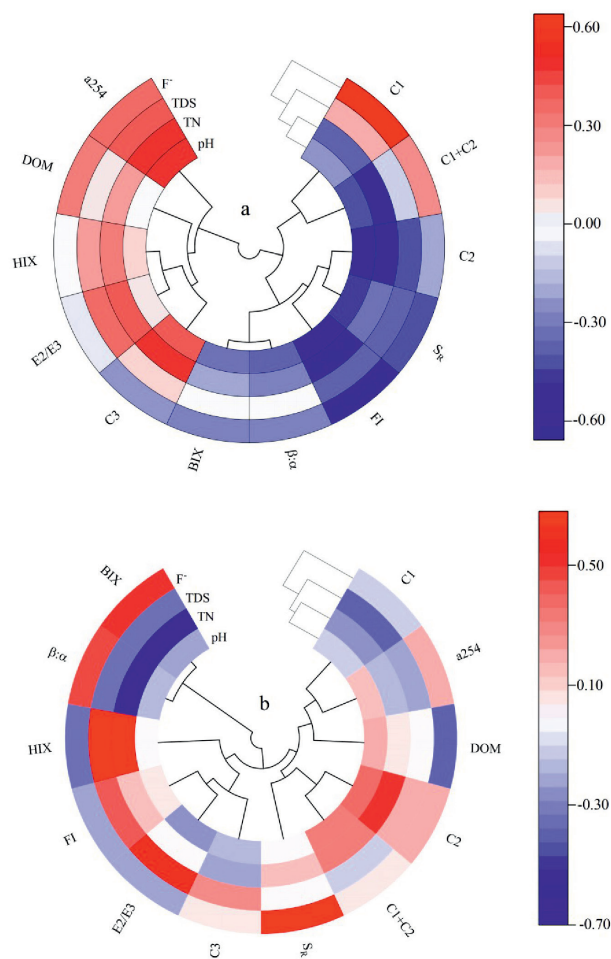


Fig. 8. Correlation between DOM components, spectral parameters and hydrochemistry: a) in shallow mine water; b) in deep mine water.

Conclusion

In the present study, the concentrations, sources, and fluorescence characteristics of DOM were compared between shallow and deep mine waters by combined analyses of EEM-PARAFAC and hydrochemistry.

In this study, DOM concentration was revealed in mine water, ranging from 0.12 mg/L to 4.90 mg/L, with a mean value of 0.93 mg/L. Moreover, the mean DOM concentration in shallow mine water was 1.36 times that in deep mine water. The EEM-PARAFAC model identified three different types of DOM fluorescent components in mine water: humic acid-like substances (low molecular weight), humic acid-like substances (high molecular weight), and protein-like components.

Compared with shallow mine water, DOM had lower degrees of humification and more freshly terrestrial substances with higher BIX and HIX values, and lower E2/E3 and a254 values in deep mine water owing to emulsion oil leakage. Environmental factors (TN and TDS) significantly correlate with DOM spectral parameters, but DOM properties were a minor contributor to pH and F⁻ in shallow and deep mine water.

With the recognition obtained, future studies could focus on the quantitative contribution of DOM to conveniently monitor changes in mine water quality. Although our findings are limited for the risks assessment of DOM in mine water resources and resident drinking within the study area, this study provides useful insights into the sustainable management and utilisation of mine water in the study area.

Acknowledgments

This work was supported by the Natural Science Foundation of Hebei Province (D2021508004), Open Fund of Key Laboratory of Mine Water Resource Utilization of Anhui Higher Education Institutes, Suzhou University (Grant No. KMWRU202101), and Open Fund of State Key Laboratory of Coal Resources and Safe Mining (Grant No. SKLCRSM22KFA03). We would like to thank Editage (www.editage.cn) for English language editing.

Conflict of Interest

The authors declare no conflict of interest.

References

- LYU L., LIU G., SHANG Y., WEN Z., HOU J., SONG K. Characterization of dissolved organic matter (DOM) in an urbanized watershed using spectroscopic analysis. *Chemosphere*. **277**, 130210, **2021**.
- MALIK A., PARVAIZ A., MUSHTAQ N., HUSSAIN I., JAVED T., REHMAN H.U., FAROOQI A. Characterization and role of derived dissolved organic matter on arsenic mobilization in alluvial aquifers of Punjab, Pakistan. *Chemosphere*. **251**, 126374, **2020**.
- JIANG T., BRAVO A.G., SKYLLBERG U., BJÖRN E., WANG D., YAN H., GREEN N.W. Influence of dissolved organic matter (DOM) characteristics on dissolved mercury (Hg) species composition in sediment porewater of lakes from southwest China. *Water Research*. **146**, 146, **2018**.
- JIANG T., SKYLLBERG U., BJÖRN E., GREEN N.W., TANG J., WANG D., GAO J., LI C. Characteristics of dissolved organic matter (DOM) and relationship with dissolved mercury in Xiaoqing River-Laizhou Bay estuary, Bohai Sea, China. *Environmental Pollution*. **223**, 19-30, **2017**.
- ZHOU Y., HE D., HE C., LI P., FAN D., WANG A., ZHANG K., CHEN B., ZHAO C., WANG Y., SHI Q., SUN Y. Spatial changes in molecular composition of dissolved organic matter in the Yangtze River Estuary: Implications for the seaward transport of estuarine DOM. *Science of The Total Environment*. **759**, 143531, **2021**.
- NILOY N.M., HAQUE M.M., TAREQ S.M. Characteristics, Sources, and Seasonal Variability of Dissolved Organic Matter (DOM) in the Ganges River, Bangladesh. *Environmental Processes*. **8**, 593, **2021**.
- CHAU K.W. Persistent organic pollution characterization of sediments in Pearl River estuary. *Chemosphere*. **64** (9), 1545, **2006**.
- ZHOU X., WANG Q., GUO Y., SUN X., LI T., YANG C. Spectroscopic characterization of dissolved organic matter from macroalgae *Ulva pertusa* decomposition and its binding behaviors with Cu(II). *Ecotoxicology and Environmental Safety*. **225**, 112811, **2021**.
- LI Y., GONG X., SUN Y., SHU Y., NIU D., YE H. High molecular weight fractions of dissolved organic matter (DOM) determined the adsorption and electron transfer capacity of DOM on iron minerals. *Chemical Geology*. **604**, 120907, **2022**.
- KULKARNI H., MLADENOV N., DATTA S. Effects of acidification on the optical properties of dissolved organic matter from high and low arsenic groundwater and surface water. *Science of The Total Environment*. **653**, 1326, **2019**.
- XU X., KANG J., SHEN J., ZHAO S., WANG B., ZHANG X., CHEN Z. EEM-PARAFAC characterization of dissolved organic matter and its relationship with disinfection by-products formation potential in drinking water sources of northeastern China. *Science of The Total Environment*. **774**, 145297, **2021**.
- RA A., MB A., BM B., MK C., LS C. Comparing the performance of three methods to assess DOM dynamics within two distinct glacierized watersheds of the tropical Andes - ScienceDirect. *Environmental Pollution*. **265**, 115052, **2020**.
- MURPHY K.R., HAMBLY A., SINGH S., HENDERSON R.K., KHAN S.J. Organic Matter Fluorescence in Municipal Water Recycling Schemes: toward a Unified PARAFAC Model. *Environmental Science & Technology*. **45** (7), 2909, **2011**.
- XU H., LI X., GUO M., LI F., YANG K., LIU X. Dissolved organic matters with low molecular weight fractions exhibit high photochemical potential for reactive oxygen formation. *Chemosphere*. **305**, 135542, **2022**.
- QIAO W., GUO H., HE C., SHI Q., ZHAO B. Molecular Evidence of Arsenic Mobility Linked to Biodegradable

- Organic Matter. *Environmental Science and Technology*. **54** (12), 7280, **2020**.
16. LI X., GUO H., ZHENG H., XIU W., HE W., DING Q. Roles of different molecular weights of dissolved organic matter in arsenic enrichment in groundwater: Evidences from ultrafiltration and EEM-PARAFAC. *Applied Geochemistry*. **104**, 124, **2019**.
 17. ARICHARDS L., DAN J., MAGNONE D., CGOODDY D., CHAMBERS L., JWILLIAMS P., DONGEN B.E., APOLYA D. Dissolved organic matter tracers reveal contrasting characteristics across high arsenic aquifers in Cambodia: A fluorescence spectroscopy study. *Geoscience Frontiers*. **10** (5), 15, **2019**.
 18. HAO C., SUN X., XIE B., HOU S. Increase in fluoride concentration in mine water in Shendong mining area, Northwest China: Insights from isotopic and geochemical signatures. *Ecotoxicology and Environmental Safety*. **236**, 113496, **2022**.
 19. XIAO W., LV X., ZHAO Y., SUN H., LI J. Ecological resilience assessment of an arid coal mining area using index of entropy and linear weighted analysis: A case study of Shendong Coalfield, China. *Ecological Indicators*. **109**, 105843, **2020**.
 20. SONG H., XU J., FANG J., CAO Z., LI T. Potential for mine water disposal in coal seam goaf: Investigation of storage coefficients in the Shendong mining area. *Journal of Cleaner Production*. **244**, 118646, **2019**.
 21. GU D., LI J., CAO Z. Technology and engineering development strategy of water protection and utilization of coal mine in China. *Journal of China Coal Society*. **46** (10), 3079, **2021**.
 22. ZHANG Z., LI G., SU X., ZHUANG X., WANG L., FU H., LI L. Geochemical controls on the enrichment of fluoride in the mine water of the Shendong mining area, China. *Chemosphere*. **284**, 131388, **2021**.
 23. ZHANG D., FANG G., MA L., WANG X. Aquifer protection during longwall mining of shallow coal seams: A case study in the Shendong Coalfield of China. *International Journal of Coal Geology*. **86** (2), 190, **2011**.
 24. CHI M.-B., LI Q.-S., CAO Z.-G., FANG J., WU B.-Y., ZHANG Y., WEI S.-R., LIU X.-Q., YANG Y.-M. Evaluation of water resources carrying capacity in ecologically fragile mining areas under the influence of underground reservoirs in coal mines. *Journal of Cleaner Production*. **379**, 134449, **2022**.
 25. ZHANG C., WANG F., BAI Q. Underground space utilization of coalmines in China: A review of underground water reservoir construction. *Tunnelling and Underground Space Technology*. **107**, 103657, **2021**.
 26. WANG Q., LI W., LI T., LI X., LIU S. Goaf water storage and utilization in arid regions of northwest China: A case study of Shennan coal mine district. *Journal of Cleaner Production*. **202**, 33, **2018**.
 27. ZHANG X., YANG J., WANG H., LIU J., DONG X., WANG T. DOM characteristics and sources of mine water in themiddle Yellow River Basin based on parallel factor method. *Journal of China Coal Society*. **46** (S2), 936, **2021**.
 28. HAN J. Analysis of the source of DOM in underground reservoir of coal mine. *Journal of Mining Science and Technology*. **5** (5), 575, **2020**.
 29. ZHAO L., SUN C., YAN P., ZHANG Q., WANG S., LUO S., MAO Y. Dynamic changes of nitrogen and dissolved organic matter during the transport of mine water in a coal mine underground reservoir: Column experiments. *Journal of Contaminant Hydrology*. **223**, 103473, **2019**.
 30. ZHONG B., WANG L., LIANG T., XING B. Pollution level and inhalation exposure of ambient aerosol fluoride as affected by polymetallic rare earth mining and smelting in Baotou, north China. *Atmospheric Environment*. **167**, 40, **2017**.
 31. GUO Y. The concentrations of F⁻, Cl⁻ and SO₄²⁻ determined by ion chromatography in drinking water of Shendong mining area. *China Chemical Trad.* **9** (10), 111, **2017**.
 32. HAO C., SUN X., PENG Y., XIE B., HE K., WANG Y., LIU M., FAN X. Geochemical impact of dissolved organic matter on antimony mobilization in shallow groundwater of the Xikuangshan antimony mine, Hunan Province, China. *Science of The Total Environment*. **860**, 160292, **2023**.
 33. KULKARNI H.V., MLADENOV N., JOHANNESSON K.H., DATTA S. Contrasting dissolved organic matter quality in groundwater in Holocene and Pleistocene aquifers and implications for influencing arsenic mobility. *Applied Geochemistry*. **77**, 194, **2017**.
 34. REN W., XIAODONG W.U., XUGUANG G.E., LIN G., ZHOU M., LONG Z., XINHUI Y.U., TIAN W. Characteristics of dissolved organic matter in lakes with different eutrophic levels in southeastern Hubei Province, China. *Journal of Oceanology and Limnology*. **39** (4), 21, **2021**.
 35. CHEN W., YU H.-Q. Advances in the characterization and monitoring of natural organic matter using spectroscopic approaches. *Water Research*. **190**, 116759, **2021**.
 36. SONG K.S., ZANG S.Y., ZHAO Y., LI L., DU J., ZHANG N.N., WANG X.D., SHAO T.T., GUAN Y., LIU L. Spatiotemporal characterization of dissolved carbon for inland waters in semi-humid/semi-arid region, China. *Hydrology and Earth System Sciences*. **17** (10), 4269, **2013**.
 37. YI B., LIU J., HE W., LÜ X., CAO X., CHEN X., ZENG X., ZHANG Y. Optical variations of dissolved organic matter due to surface water - groundwater interaction in alpine and arid Datonghe watershed. *Science of The Total Environment*. **864**, 161036, **2023**.
 38. DU L., LIU Y., HAO Z., CHEN M., LI L., REN D., WANG J. Fertilization regime shifts the molecular diversity and chlorine reactivity of soil dissolved organic matter from tropical croplands. *Water Research*. **225**, 119106, **2022**.
 39. LYU L., WEN Z., JACINTHE P.-A., SHANG Y., ZHANG N., LIU G., FANG C., HOU J., SONG K. Absorption characteristics of CDOM in treated and non-treated urban lakes in Changchun, China. *Environmental Research*. **182**, 109084, **2020**.
 40. XIE H., AUBRY C., BÉLANGER S., SONG G. The dynamics of absorption coefficients of CDOM and particles in the St. Lawrence estuarine system: Biogeochemical and physical implications - ScienceDirect. *Marine Chemistry*. **s128–129** (1), 44, **2012**.
 41. SUN Y., LAN J., CHEN X., YE H., DU D., LI J., HOU H. High arsenic levels in sediments, Jiangnan Plain, central China: Vertical distribution and characteristics of arsenic species, dissolved organic matter, and microbial community. *Journal of Geochemical Exploration*. **228**, 106822, **2021**.
 42. PI K., WANG Y., XIE X., HUANG S., YU Q., YU M. Geochemical effects of dissolved organic matter biodegradation on arsenic transport in groundwater systems. *Journal of Geochemical Exploration*. **149**, 8, **2015**.
 43. GUO H., LI X., XIU W., HE W., CAO Y., ZHANG D., WANG A. Controls of organic matter bioreactivity on arsenic mobility in shallow aquifers of the Hetao Basin, P.R. China. *Journal of Hydrology*. **571**, 448, **2019**.

44. LI W., JIA X., LI M., WU H. Insight into the vertical characteristics of dissolved organic matter in 5-m soil profiles under different land-use types on the Loess Plateau. *Science of The Total Environment*. **692**, 613, **2019**.
45. MAQBOOL T., SUN M., CHEN L., ZHANG Z. Molecular-level characterization of natural organic matter in the reactive electrochemical ceramic membrane system for drinking water treatment using FT-ICR MS. *Science of The Total Environment*. **846**, 157531, **2022**.
46. ZHAO L., TIAN Y., WANG S., SUN Y., LUO S. Dynamic changes of dissolved organic matter (DOM) from coal gangue. *Journal of China Coal Society*. **42** (9), 2455, **2017**.
47. PARLANTI E., WÖRZ K., GEOFFROY L., LAMOTTE M. Dissolved organic matter fluorescence spectroscopy as a tool to estimate biological activity in a coastal zone submitted to anthropogenic inputs. *Organic Geochemistry*. **31** (12), 1765, **2000**.
48. YANG X., YUAN J., YUE F.-J., LI S.-L., WANG B., MOHINUZZAMAN M., LIU Y., SENESI N., LAO X., LI L., LIU C.-Q., ELLAM R.M., VIONE D., MOSTOFA K.M.G. New insights into mechanisms of sunlight- and dark-mediated high-temperature accelerated diurnal production-degradation of fluorescent DOM in lake waters. *Science of The Total Environment*. **760**, 143377, **2021**.
49. LIU D., DU Y., YU S., LUO J., DUAN H. Human activities determine quantity and composition of dissolved organic matter in lakes along the Yangtze River. *Water Research*. **168**, 115132, **2020**.
50. CHENG Y., ZHAO K., ZHANG Y., ZHANG Y., JIAO L. Fluorescence Spectral Characteristics of Dissolved Organic Matter in Songhua Lake Sediment. *Environmental Sciences*. **43** (04), 1941, **2022**.
51. CHEN B., ZHAO M., LIU C., FENG M., MA S., LIU R., CHEN K. Comparison of copper binding properties of DOM derived from fresh and pyrolyzed biomaterials: Insights from multi-spectroscopic investigation. *Science of The Total Environment*. **721**, 137827, **2020**.